CLM - P 576

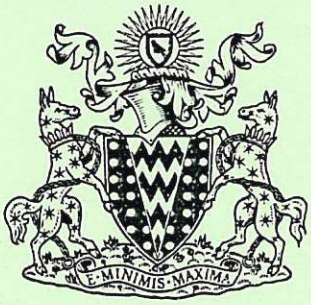

UKAEA

Preprint

ON THE MUTUAL INTERACTION BETWEEN ROTATION AND MAGNETIC FIELDS FOR AXISYMMETRIC BODIES

C G GIMBLETT
R S PECKOVER

CULHAM LABORATORY
Abingdon Oxfordshire

1979

CLM-P 576

ON THE MUTUAL INTERACTION BETWEEN ROTATION AND MAGNETIC FIELDS FOR AXISYMMETRIC BODIES

C G Gimblett and R S Peckover

UKAEA Culham Laboratory,

Abingdon, Oxon. OX14 3DB

(To be published in Proc. Roy. Soc.)

ABSTRACT

As a simple example of the mutual interaction between magnetic fields and material motions, the rotation of an electrically conducting cylinder of solid material in a transverse magnetic field has been investigated. An applied driving torque produces the rotation which is opposed by friction and the induced magnetic torque. It is well known that when the field is transverse to the rotation axis the magnetic torque rises from zero as the rotation rate Ω is increased, reaches a maximum and tends to zero as $\Omega \to \infty$, and the magnetic flux is expelled. We may consider B_o (the applied magnetic field strength) and Ω_o (the rotation rate at which the drive is just balanced by friction alone) as control parameters of the system. For sufficiently strong driving torques, the equilibrium surface $\Omega(\Omega_o, B_o)$ develops a fold and consists of two branches - 'fast friction-dominated' and 'slow magnetically-dominated' stable rotation rates. These solutions embrace an unstable intermediate equilibrium, and the system exhibits hysteresis depending on the manner in which the fold is approached. A 'potential' function can be introduced in terms of which the equilibria and stability can be analysed, and this potential function indicates that the equilibrium Ω-surfaces display the characteristics of the cusp catastrophe of Thom. One consequence of this folded structure is the existence of a forbidden band of rotation rates for a given driving torque irrespective of magnetic field strength. Similar properties can be shown for spheres, and we speculate that the general features - fold, upper and lower stable branches, forbidden band of stable rotation rates - are generic to all axisymmetric solid bodies and shells rotating about their axes of symmetry in the presence of a magnetic field with a transverse component. These features are absent if the magnetic field is aligned with the rotation axis. The hysteresis should be observable in the laboratory and experimentally verifiable.

October 1978

1. INTRODUCTION

The kinematic advection of magnetic fields due to the inductive effect of a moving electrical conductor is a well known phenomenon. However the full dynamic interaction between magnetic fields and moving media, in which the induced fields can alter the conductor's motion, is perhaps less well understood. In this paper we consider some particular systems for which this interaction can be fairly thoroughly analysed.

We investigate the rotation of an electrically conducting cylinder in a transverse magnetic field. A steady driving torque is the source of the rotation which is opposed by both an applied frictional torque and the induced magnetic torque. The rotation of the cylinder about its axis is entirely specified by one parameter - the angular velocity - and we examine the dynamic relationship between this parameter and the magnetic field configuration.

Much of the earlier work on induction in solid rotators was motivated by problems in geomagnetism, in particular the problem of the origin of the terrestrial magnetic field (e.g. Bullard 1949, Herzenberg and Lowes 1957, R L Parker 1966). The electromagnetic generation of centrifugal flow by applying rotating or alternating magnetic fields to cylinders containing liquid metals provides an almost equivalent problem, and a number of analyses of limiting cases have been carried out (Moffatt 1964, Devanthan and Bhatnagar 1967, Dahlberg 1972 and the references therein, Richardson 1974). Interest in the concentration of magnetic fields at the granular and supergranular boundaries of the solar photosphere has resulted in studies of the kinematic expulsion of magnetic flux by eddies (E.N. Parker 1963, Clark 1965, Weiss 1964, 1966) and the dynamic (non-turbulent) interaction between magnetic fields and convection has been examined to some extent (Busse 1975, Peckover and Weiss 1978, Galloway, Proctor, Weiss 1977, 1978). The rotation of plasma in a θ-pinch has been analysed in terms of a driving torque produced by an axial Hall current, and an opposing magnetic torque arising from the rotation in a transverse magnetic field (Thonemann and Kolb 1964).

We consider a solid annular cylinder of outer radius a rotating about its principal axis with angular velocity Ω in the presence of a constant applied transverse magnetic field of strength B_o. The rotation is opposed by a frictional torque taken to be proportional to Ω (to model some of the effects of viscosity) and is produced by a constant driving torque which can be characterised by the angular velocity Ω_o for which the drive is just balanced by friction. The rotation also induces a retarding magnetic torque which for transverse fields increases with Ω to a maximum value and then decreases

ultimately to zero as the flux is expelled (Bullard 1949).

Considering Ω_o and B_o as "control variables", we have examined the possible equilibrium values for Ω in the two limiting cases of a completely solid cylinder, and a thin cylindrical shell and find that in both cases, the equilibrium surfaces display the characteristics of the cusp catastrophe of Thom (1975). For sufficiently strong driving torques, the equilibrium surface $\Omega(\Omega_o,B_o)$ develops a fold and consists of two branches. The upper and lower branches are found to represent stable equilibria, and for one given point in (Ω_o,B_o) space the system can in principle adopt either equilibrium. These "fast" and "slow" stable solutions embrace an unstable intermediate equilibrium, and the system can exhibit hysteresis with the transition from one equilibrium to the other depending on the manner in which the fold is approached.

The analysis of the equilibria and their linear stability properties is facilitated by introducing a 'potential' function to describe the system. In none of the cases we study is the form of this potential a simple polynomial, but the topological properties of each function certainly indicate a cusp-type catastrophe in each instance. Similar properties can be shown for solid spheres, and we speculate that this behaviour is generic to all axisymmetric solid bodies and shells rotating about their axis of symmetry in the presence of a transverse applied magnetic field.

In §2 we derive equations describing the magnetic stream function, angular momentum and magnetic torque for a general cylindrical annulus. The completely solid cylinder is then considered in §3 and we obtain its equilibria. The corresponding dispersion relation is derived and used to examine the linear stability characteristics. The thin annulus investigated in §4 gives a simpler problem mathematically, and a full stability analysis can be carried out.

The analysis of this paper often makes use of complex functions to represent the physical variables, and it is well known that care has to be taken to specify real and imaginary parts where used (especially when calculating quadratic quantities such as magnetic torque). Where real or imaginary parts are intended the symbols $\mathcal{R}e$ or $\mathcal{I}m$ are used explicitly; otherwise the full complex quantity is implied.

2. GENERAL FORMULATION

2.1 Configuration and Equations

We consider the problem of a right circular solid annular cylinder of mass M, length L, outer radius a, and inner radius ka, rotating in vacuo about its principal axis. The rotation takes place in a transverse applied uniform magnetic field of strength B_o maintained by sources at infinity. We neglect end effects and, taking L >> a, can expect close two-dimensionality in the system. The cylinder rotation induces a current and hence a magnetic torque $\mathcal{M}$. For convenience we imagine the current flow to be closed by a suitably arranged external circuit which interferes in no other way with the system. The rotation is assumed to be driven by a steady applied torque $\mathcal{T}$, and opposed by a frictional torque $\mathcal{L}$ taken to be proportional to the instantaneous rate of rotation. In this section we derive and partially solve the equations which control the motion of this solid annular cylinder; in the two subsequent sections we consider in detail two limiting cases:- firstly in §3 the solid cylinder (k = 0), which provided the original motive for examining this system, and secondly in §4 the thin annular cylindrical shell (k ≃ 1), which is more tractable analytically and shows the essential features in a clearer fashion.

The equations that govern the magnetic induction $\underline{B}$ are

$$\frac{\partial \underline{B}}{\partial t} = \text{curl}\ (\underline{v} \wedge \underline{B}) + \eta \nabla^2 \underline{B}\ , \tag{2.1}$$

within the solid cylindrical material, and

$$\text{curl}\ \underline{B} = \underline{0}\ , \tag{2.2}$$

in vacuo, subject in both cases to the solenoidal condition

$$\text{div}\ \underline{B} = 0\ . \tag{2.3}$$

Here t is the time, $\underline{v}$ is the cylinder velocity, and the uniform and constant magnetic diffusivity η is given by $(\mu\sigma)^{-1}$ where μ and σ are the cylinder permeability and conductivity respectively.

The angular momentum equation for the cylinder is

$$I \frac{d\Omega}{dt} = \mathcal{T} - \mathcal{L} + \mathcal{M}\ , \tag{2.4}$$

where $\Omega(t)\hat{\underline{Z}}$ is the angular velocity of the cylinder using cylindrical polar

co-ordinates R,θ,Z in the normal way, and $I = \frac{1}{2} Ma^2(1 + k^2)$ is the moment of inertia. Equations (2.1) to (2.4) together with appropriate initial and boundary conditions form a complete set for the evolution of the magnetic field and angular velocity.

2.2 The Magnetic Field and Magnetic Torque

Since it is assumed here that all variables are independent of the axial co-ordinate Z, a vector potential $\underline{A} = A(R,\theta,t)\hat{\underline{Z}}$ may be introduced for the induction $\underline{B}$. We have then

$$\underline{B} = \text{curl } \underline{A} = \frac{1}{R}\frac{\partial A}{\partial \theta}\,\hat{\underline{R}} - \frac{\partial A}{\partial R}\,\hat{\underline{\theta}}\,, \tag{2.5}$$

so that (2.3) is automatically satisfied.

It is convenient to introduce dimensionless variables r,z,ω,τ and α by $R = ar, Z = Lz, \Omega = \Omega_\eta \omega$, $t = \Omega_\eta^{-1}\tau$, and $A = B_o a\alpha$ where $\Omega_\eta^{-1} = a^2(1 - k^2)\eta^{-1}$. The dimensionless angular velocity ω is then effectively the magnetic Reynolds number for the system.

Substituting (2.5) into (2.1) and (2.2) we can perform an integration to give, in non-dimensional variables, the following equation for α (assuming no externally applied electric field):

$$\frac{\partial \alpha}{\partial \tau} + \omega \frac{\partial \alpha}{\partial \theta} = (1 - k^2)\nabla^2\alpha, \quad k \leq r \leq 1\,, \tag{2.6}$$

$$\nabla^2\alpha = 0\,, \quad 0 \leq r \leq k \text{ and } r \geq 1\,. \tag{2.7}$$

In general, α can be expressed as an infinite sum of cylindrical harmonics of the form $f_m(r,\tau)e^{im\theta}$. However we need only be concerned with the $m = 1$ component (see Appendix 1) and can write α as

$$\left.\begin{aligned} \alpha &= \mathcal{R}e\{(r + b(\tau)/r)e^{i\theta}\}\,, \quad r \geq 1\,, \\ &= \mathcal{R}e\{\quad c(\tau)re^{i\theta}\quad\}\,, \quad 0 \leq r \leq k\,, \\ &= \mathcal{R}e\{\quad D(r,\tau)e^{i\theta}\quad\}\,, \quad k \leq r \leq 1\,, \end{aligned}\right\} \tag{2.8}$$

where b, c and D are in general complex. The boundary conditions can be

put in the convenient form

$$(\alpha - r \frac{\partial \alpha}{\partial r})_{r=k} = 0 \ , \tag{2.9}$$

and

$$(\alpha + r \frac{\partial \alpha}{\partial r})_{r=1} = 2 \mathcal{R}e\,(e^{i\theta}) \ , \tag{2.10}$$

(see R.L.Parker 1966)*.

Condition (2.10) implies

$$\mathcal{I}_m [D^* \frac{dD}{dr}]_{r=1} = - 2 \mathcal{I}_m [D]_{r=1} \ , \tag{2.11}$$

which enables the magnetic torque (A.3) to be written as

$$\mathcal{M} = \frac{2\pi B_o{}^2 La^2}{\mu} [\beta_2]_{r=1} \ , \tag{2.12}$$

where $D \equiv \beta_1(r,\tau) + i\beta_2(r,\tau)$ with β_1, β_2 real functions. To give $[\beta_2]_{r=1}$ physical content we note that on $r = 1$ when $\theta = 0$ or π, the magnitude of the radial magnetic field is $B_o[\beta_2]_{r=1}$. Further, the magnetic flux crossing the diametral plane $\theta = \frac{\pi}{2}$ within the cylinder is $2B_o aL[\beta_2]_{r=1}$.

2.3 The Angular Momentum

Let us express the frictional torque $\mathcal{L}$, which is by hypothesis proportional to the angular velocity Ω, as

$$\mathcal{L} = \lambda M \Omega \ , \tag{2.13}$$

where λ is a coefficient of friction with dimension $[L^2 T^{-1}]$. In the absence of magnetic field, a steady angular velocity Ω_o will be attained in which the driving torque balances friction; hence $\mathcal{J} = \lambda M \Omega_o$. The equation of angular momentum for the cylindrical annulus can thus be written in non-dimensional form as

$$p^{-1} \frac{d\omega}{d\tau} = \omega_o - \omega + \tfrac{1}{2} Q \beta_2 (1,\tau) \ , \tag{2.14}$$

where the coupling parameter Q is given by

$$Q = \frac{4B_o{}^2 a^2}{\mu \rho \lambda \eta} \ , \tag{2.15}$$

---

* $\theta = \frac{-\pi}{2}$ gives the direction of the externally applied magnetic field.

and ρ is the uniform density of the cylinder material. The quantity Q can be recognised as a modified Chandrasekhar number* (see, e.g. Weiss 1964), with λ playing the role of kinematic viscosity, and p is a modified magnetic Prandtl number given by

$$p = \frac{2(1 - k^2)}{(1 + k^2)} \frac{\lambda}{\eta} . \qquad (2.16)$$

2.4 Steady Rotation

When the rotation rate has reached an equilibrium value, equation (2.14) becomes $f(\omega) = 0$ where

$$f(\omega) \equiv \omega_o - \omega + \tfrac{1}{2} Q\beta_2(1) , \qquad (2.17)$$

and β_2 at $r = 1$ has been evaluated from the time-independent solution of (2.6). In representing such equilibria it is convenient to introduce a potential function 'ψ' such that

$$f(\omega) = - \frac{\partial \psi}{\partial \omega} . \qquad (2.18)$$

The roots of $f(\omega) = 0$, representing the steady state of the system, then correspond to turning points of the potential ψ.

---

*The Chandrasekhar number Q may be more familiar as H^2 where H is the Hartmann number.

3. THE SOLID CYLINDER

When k = 0, the annular cylinder becomes a complete solid cylinder, and the inner harmonic region for A disappears. However, the magnetic torque is still given by (2.12) and equations (2.6) and (2.14) control the system. The moment of inertia I is $\frac{1}{2} Ma^2$, the dimensionless angular velocity ω (the magnetic Reynolds number) reduces to $\Omega a^2/\eta$, while p becomes $2\lambda/\eta$.

3.1 Steady Rotation

In this subsection we concentrate primarily on the possible equilibria of the system. Putting all time derivatives equal to zero, it is straightforward to solve for the magnetic field (see Gimblett 1977 , Landau and Lifschitz 1960):

$$\alpha = \mathcal{R}e \left[\frac{2J_1(qr)}{qJ_o(q)} e^{i\theta}\right] , \quad r \leqslant 1 , \tag{3.1}$$

$$= \mathcal{R}e \left[\left(r + \frac{J_2(q)}{rJ_o(q)}\right) e^{i\theta}\right] , \quad r \geqslant 1 , \tag{3.2}$$

where $q^2 = -i\omega$ and J_n denotes the Bessel function of the first kind of order n. The form of (3.2) shows that the external field can be regarded as the sum of a uniform field and an induced dipole field (see e.g. Bullard 1949).

It follows that the magnetic torque $\mathcal{M}$ (Eq. (2.12)) is

$$\mathcal{M} = \frac{4\pi B_o{}^2 La^2}{\mu} \mathcal{I}m \left[\frac{J_1(q)}{qJ_o(q)}\right] . \tag{3.3}$$

A full discussion of the properties of expression (3.3) is given in Gimblett (1977). A graph of the magnetic torque against ω is shown in Fig. 1. An interesting feature of this curve is the maximum value of $\mathcal{M}$ appearing at $\omega \simeq 6.3$. For values of ω above this value, there is a gradual decrease in the braking effect of the field (see §5 where the physical basis for this effect is discussed). The occurrence of this maximum value has important implications for the family of equilibria the system can adopt as we have shown that in certain regimes, one value of the retarding magnetic torque can correspond to two distinct rotation rates.

Returning to the equilibrium problem, we recall that the dynamic balance is now given by

$$f(\omega) \equiv \omega_o - \omega + Q \mathcal{I}m \left[\frac{J_1(q)}{qJ_o(q)}\right] = 0 , \quad q^2 = -i\omega , \tag{3.4}$$

where the torque $\leqslant 0$, tending to zero for $\omega \to 0$ and $\omega \to \infty$.

Equation (3.4) defines ω as an implicit function of ω_o and Q. These latter

two parameters are determined by external agencies and can be thought of as the 'control variables' of the system. Fig. 2 shows the locus of equilibrium values of ω plotted against Q for various values of ω_o. For $\omega_o > 42.34$, there are three distinct possible equilibria for any one given value of Q. To obtain a graphic representation of these equilibria, we can form a potential function ψ as in (2.18). Using

$$\mathfrak{Im}\left[\frac{J_1(q)}{qJ_o(q)}\right] = -\frac{\partial}{\partial\omega}\,\ell n\left[\mathrm{ber}^2(\omega^{\frac{1}{2}}) + \mathrm{bei}^2(\omega^{\frac{1}{2}})\right], \tag{3.5}$$

we obtain the potential in the form

$$\psi(\omega) = \tfrac{1}{2}\,\omega^2 - \omega\omega_o + Q\,\ell n\,[\mathrm{ber}^2(\omega^{\frac{1}{2}}) + \mathrm{bei}^2(\omega^{\frac{1}{2}})]. \tag{3.6}$$

(For definitions of the Kelvin functions ber and bei, see for example Tranter 1968 p.22).

3.2 Stability

The question now naturally arises as to which (if any) of the equilibria found in the previous subsection are stable to small perturbations. To determine the linear stability properties of the system, it is necessary to reinstate the time derivatives of Eqs. (2.6) and (2.14), and assuming small perturbations about an equilibrium we can write (for example) $\omega = \omega_e + \mathfrak{Re}\,(\tilde{\omega}e^{\gamma\tau})$, where the e subscript indicates an equilibrium value, and $\tilde{\omega}$ and γ are the perturbation amplitude and growth rate respectively. The magnetic field is similarly perturbed, with care being taken to distinguish between real and complex quantities. From the discussion in the Appendix, we need consider only perturbations with m = 1, as the rest do not contribute to the torque. Substituting into the linearized perturbation equations, we first solve for the magnetic field and then calculate the perturbed magnetic torque. The resulting dispersion relation is

$$(p^{-1}\gamma + 1) = \frac{Q}{2\gamma}\left[\frac{J_1(k_1)}{k_1J_o(k_1)} + \frac{J_1(k_2)}{k_2J_o(k_2)} - 2\,\mathfrak{Re}\left\{\frac{J_1(q)}{qJ_o(q)}\right\}\right], \tag{3.7}$$

where

$$k_1^2 = -\gamma + q^2\,,\quad k_2^2 = -\gamma - q^2\,,\quad \text{and } q^2 = -i\omega_e\,.$$

First we consider the stability of the system to what Herzenberg and Lowes (1957) term 'adiabatic' perturbations (i.e. perturbations in which the magnetic field configuration is assumed to adjust itself instantaneously to any small change in the angular velocity). The dispersion relation for this system can be obtained either by a linearisation of (2.14) or equivalently by taking $\underset{\gamma\to 0}{\text{Lt}}$ of the R.H.S. of (3.7). The adiabatic assumption is then seen to correspond to $p \ll 1$. We find that the growth rate of adiabatic perturbations, γ_A, is real and given by:

$$\gamma_A = -p\left[1 + Q\,\mathcal{R}e\left\{\frac{d}{d(q^2)}\left(\frac{J_1(q)}{qJ_o(q)}\right)\right\}\right] . \tag{3.8}$$

Recalling that

$$\frac{\partial\psi}{\partial\omega} = \omega - \omega_o - Q\,\mathcal{I}m\left[\frac{J_1(q)}{qJ_o(q)}\right] ,$$

it follows that

$$\gamma_A = -p\,\partial^2\psi/\partial\omega^2 . \tag{3.9}$$

The adiabatic stability of the equilibria, then, is directly related to the sign of ψ'' at the points $\psi' = 0$. In fact, stable equilibria correspond to minima in ψ, and unstable equilibria to maxima. Furthermore, the points of marginal stability $\psi'' = 0$ correspond to the turning points $\partial Q/\partial\omega = 0$ (when they exist) in Fig. 2 (this follows easily on differentiating (3.4) with respect to ω with $d/d\tau \equiv 0$).

Fig. 3a shows plots of ψ for $\omega_o = 75$ and three values of Q. The three curves shown represent values of ψ for cross-sectional cuts in the graph of ω against Q shown in Fig. 3b . Curve A exhibits one adiabatically stable equilibrium, B possesses two stable equilibria separated by an unstable one, while C again has one stable equilibrium. When three equilibria are present for fixed values of ω_o and Q, the "fast" and "slow" types are adiabatically stable, and they embrace an unstable intermediate equilibrium.

The dispersion relation (3.7) has also been examined for general p. One can easily show that the roots of (3.7) for γ are either real or occur as conjugate complex pairs. Numerical studies indicate that there are in fact three roots, at least one of which is always real (c.f. §4.3). The real root is zero only when $\psi_{\omega\omega} = 0$. Moreover when γ is real and small

$$p^{-1}\gamma = -\frac{\psi_{\omega\omega}}{(1+\frac{1}{2}pQX)} + O(\gamma^2) \quad , \tag{3.10}$$

where $X = \frac{d^2}{d\omega^2}\mathcal{Re}(Y)$ with $Y = \frac{J_1(q)}{qJ_o(q)}$. A graph of $\mathcal{Re}(Y)$ as a function of ω shows that X is positive for $\omega > 3.1$. However for γ sufficiently small, $\psi_{\omega\omega} \simeq 0$ which implies $\frac{d}{d\omega}\mathcal{Im}(Y) \simeq -Q^{-1}$. As Fig. 1 indicates $\mathcal{Im}(Y)$ can only have a negative gradient for $\omega > 6.3$. It follows that in the vicinity of the turning points the real root γ and $\psi_{\omega\omega}$ have opposite signs. Numerical studies of the conjugate complex pair of roots $\gamma_1 \pm i\gamma_2$ show that γ_1 is negative for the whole range of parametric choice. It follows that the condition $\psi_{\omega\omega} \gtrless 0$ is indeed the stability discriminant for general values of p. Figure 4 shows the real root and the real and imaginary parts of the complex roots for γ as ω varies between 0 and ω_o on the equilibrium curve for $\omega_o = 100$ and $p = 1$. The real root is positive for $6.9 < \omega < 29.7$, where $\psi_{\omega\omega} < 0$.

We have thus demonstrated that the behaviour characteristic of the solid cylinder when $p \ll 1$ is present irrespective of the value of p; certainly in the more tractable case of the thin annular shell analysed in the next section we prove rigorously that the stability characteristics hold independent of the value of p.

3.3 Behaviour of Equilibria in the (ω_o - Q) Control Space

It is now quite clear that the system described in §3.2 possesses a simple cusp catastrophe (Thom 1975), and will display the well-known characteristics associated with it. For example, imagine holding ω_o fixed at 75, and slowly increasing Q by increasing the ambient field strength B_o (see Fig. 3b). The system will remain stably in a rapidly rotating equilibrium up to $Q \simeq 415.7$, where we expect a 'discontinuous' jump in the angular velocity ω down to the slowly rotating equilibrium corresponding to the same value of Q. This event corresponds in Fig. 3a to the disappearance of the right hand stable equilibrium between curves B and C. Slowly decreasing the field strength from this value, the system follows the stable path in Fig. 3b back to $Q \simeq 361.7$ where a (larger) jump in ω will restore the system to the corresponding fast equilibrium, corresponding to the disappearance of the left hand stable equilibrium between curves B and A in Fig. 3a. Such hysteresis is a basic feature of the cusp catastrophe, and defines a 'forbidden' regime for each fixed ω_o in which there is no stable equilibrium for a range of values of ω. The forbidden zone of Fig. 3b, for example, is $7.2 \lesssim \omega \lesssim 22.3$.

Figure 5 shows a three-dimensional plot of the developing fold in (ω_o, Q, ω) space. The 'pucker point' I occurs at $\omega_I \simeq 10.7$, $\omega_{oI} \simeq 42.3$, $Q_I \simeq 185.1$.

4. THE ANNULAR SHELL

Analysis of the conducting solid cylinder rotating in a steady transverse applied magnetic field leads to expressions involving Bessel functions of complex or at least semi-imaginary argument which cannot be manipulated in a straight forward manner. A mathematically simpler problem with the same essential features is that for which the rotating cylinder is a hollow shell of circular cross-section.

We take the shell to have thickness $\delta \ll a$. The analysis of §2 for the general annulus still applies, but the magnetic stream function A can be considered to be independent of r within the shell. An examination of the limiting process $\delta/a \to 0$ shows this to be justified for sufficiently small δ/a.

Neglecting $O(\delta/a)^2$, we find, since $k = 1 - \delta/a$, that the mass of the shell is now $2\pi\rho La\delta$, its moment of inertia I is Ma^2, the modified Prandtl number p becomes $2(\frac{\delta}{a})(\lambda/\eta)$ and the non-dimensional angular velocity ω (effectively the magnetic Reynolds number) is $2a\delta\Omega/\eta$.

4.1 The Magnetic Field

With the assumption that the shell is negligibly thin, the vacuum field is given by

$$\left.\begin{aligned} \alpha &= \mathcal{R}e\ \{(1 + C)re^{i\theta}\} \quad r < 1 , \\ &= \mathcal{R}e\ \{(r + C/r)e^{i\theta}\},\ r > 1 , \end{aligned}\right\} \tag{4.1}$$

and within the shell the induced component of the field is given by

$$\alpha_1 = \mathcal{R}e\{Ce^{i\theta}\} , \tag{4.2}$$

where $C = C(\tau)$.

The (axial) current density j for the induced eddy currents can be calculated from the jump in the tangential component of the induced magnetic field across the shell, assuming the radial distribution of j is constant over the thickness δ:

$$j\delta = \mu^{-1}\left[-\frac{\partial A}{\partial R}\right]_{int}^{ext} = +\ 2B_o\alpha_1/\mu . \tag{4.3}$$

Since $\nabla^2 A = -\mu j$ a little manipulation puts equation (2.6) into the form

$$\frac{dC}{d\tau} + i\omega(1 + C) + 4C = 0 . \tag{4.4}$$

4.2 Steady Rotation

As in §3 we now obtain the equilibria corresponding to steady rotation rates, and examine their stability. Unlike the analysis for the solid cylinder, this can be done completely and explicitly.

In equilibrium $C = -i\omega/(4 + i\omega)$, so that $\beta_2(1) = \Im m(C) = -4\omega/(16 + \omega^2)$. Inserting this in (2.17) we obtain an equation for the steady dimensionless rotation velocity ω in terms of the control parameters ω_o and Q:

$$f(\omega) \equiv \omega_o - \omega - \frac{2Q\omega}{16 + \omega^2} = 0 \ , \tag{4.5}$$

(cf. equation (3.4)). This equation for ω is a cubic equation with real coefficients, and so has either one or three real solutions depending on the values of the control parameters. Note that the magnetic torque term in (4.5) has exactly the same form as the simple torque/slip equation of an induction motor (see e.g. Jayawant 1968 , pp.69 - 73).

As for the case of the solid cylinder, we can form a potential function ψ satisfying (2.18). This potential, whose turning points represent the equilibria of the system, has the form

$$\psi(\omega) = \tfrac{1}{2}\omega^2 - \omega\omega_o + Q \ \ell n \ (16 + \omega^2). \tag{4.6}$$

Qualitatively this potential looks very similar to the solid cylinder potential (see for example fig. 3a). Figure 6 shows a schematic representation of $f(\omega) = 0$, for the different regimes of the annular cylindrical shell. The three curves shown are the equilibria curves $\omega = \omega(Q)$ for different values of ω_o. For $\omega << 4$, (4.5) reduces to $\omega = \omega_o/(1 + 2Q)$ so that $\omega \sim Q^{-1}$. If $\omega_o < \omega_{oI}$, ω is a monotonic decreasing function of Q (see curve (iii) in Fig. 6). If $\omega_o > \omega_{oI}$, a re-entrant 'knee' develops in the curve $\omega = \omega(Q)$ (see curve (i) in Fig. 6) These two regimes for ω_o are separated by the curve (ii) which has a point of inflexion I with infinite gradient. At I the three roots of the cubic coalesce and the cubic has the form $(\omega - \omega_I)^3 = 0$. Comparison of coefficients with (4.5) indicates that at I

$$\omega_I = 4\sqrt{3}, \ \omega_{oI} = 12\sqrt{3}, \ Q_I = 64 \ . \tag{4.7}$$

Now since for constant ω_o, $\left.\frac{\partial f}{\partial Q}\right|_\omega \cdot \frac{dQ}{d\omega} = -\left.\frac{\partial f}{\partial \omega}\right|_Q$, then

$$-2\omega \frac{dQ}{d\omega} = (16 + \omega^2) \frac{\partial^2 \psi}{\partial \omega^2} \ . \tag{4.8}$$

in which

$$\frac{\partial^2 \psi}{\partial \omega^2} = 1 - 2Q \frac{\omega^2 - 16}{(\omega^2 + 16)^2} \quad . \tag{4.9}$$

Hence the turning points Z_1 and Z_2 in figure 6 where $\frac{dQ}{d\omega} = 0$ correspond to where $\psi_\omega = \psi_{\omega\omega} = 0$ simultaneously. Inspection of equation (4.9) shows that no turning points can occur when $\omega < 4$. When ω_o is large, then Z_1 and Z_2 have (Q,ω) co-ordinates of approximately $(\omega_o^2/8 \ , \ \tfrac{1}{2} \omega_o)$ and $(4 \omega_o \ , \ 4 + 16/\omega_o)$ respectively.

4.3 Stability

To examine the stability of the dynamic equilibria of the hollow annular shell we return to the time dependent equations viz.

$$\left.\begin{aligned} p^{-1} \frac{d\omega}{d\tau} &= \omega_o - \omega + \tfrac{1}{2} Q\beta_2 \ , \\ \frac{d\beta_1}{d\tau} &+ 4\beta_1 - \omega\beta_2 = 0 \ , \\ \frac{d\beta_2}{d\tau} &+ 4\beta_2 + \omega(1 + \beta_1) = 0 \ , \end{aligned}\right\} \tag{4.10}$$

where $C(t) \equiv \beta_1 + i\beta_2$.

If an equilibrium $(\omega, \beta_1, \beta_2)_e$ - where the subscript e stands for equilibrium - is given a small perturbation such that $(\omega, \beta_1, \beta_2) = (\omega, \beta_1, \beta_2)_e + \mathcal{R}e\{(\tilde{\omega} e^{\gamma\tau}, \tilde{\beta}_1 e^{\gamma\tau}, \tilde{\beta}_2 e^{\gamma\tau})\}$ where $\tilde{\omega}$, $\tilde{\beta}_1$, $\tilde{\beta}_2$ and γ are in general complex, then the resulting dispersion relation is

$$(p^{-1}\gamma + 1)\,([\gamma + 4]^2 + \omega_e^2) + 2S(16 + 4\gamma - \omega_e^2) = 0 \ , \tag{4.11}$$

where $S = Q/(16 + \omega_e^2)$ and ω_e is an equilibrium value for ω. This dispersion relation is cubic in γ with real coefficients, and can be recast as

$$F_1(\gamma) \equiv \gamma^3 + \sigma_1\gamma^2 + \sigma_2\gamma + \sigma_3 = 0 \ , \tag{4.12}$$

where σ_1 and σ_2 are real and positive and σ_3 is real and equal to $p(16 + \omega_e^2)\psi_{\omega\omega}$. There are only two cases to be considered: <u>either</u> the cubic has three real roots $\gamma_1, \gamma_2, \gamma_3$, <u>or</u> it has one real root γ_1 and a conjugate complex pair $g_1 \pm g_2$.

(a) <u>3 real roots</u>. If $\sigma_3 > 0$, then $F_1(\gamma) > 0$ for $\gamma > 0$; hence no positive roots - the system is stable. Now $-\sigma_3$ is $\gamma_1\gamma_2\gamma_3$, the product of the roots. If $\sigma_3 < 0$ then $\gamma_1\gamma_2\gamma_3 > 0$; hence at least one positive root - the system is unstable.

(b) 1 real, 2 complex roots. One can show that $-2g_1[(g_1 - \gamma_1)^2 + g_2^2] \equiv \sigma_1\sigma_2 - \sigma_3$ which for this system is strictly positive. Hence $g_1 < 0$ and the two oscillatory modes are always damped. Also $\sigma_3 = -\gamma_1(g_1^2 + g_2^2)$. Hence $\text{sgn}(\gamma_1) = -\text{sgn}(\sigma_3)$.

In either case $\sigma_3 > 0$ gives stability, $\sigma_3 < 0$ gives instability. Thus the necessary and sufficient condition that the system is stable at its equilibria is

$$\frac{\partial^2\psi}{\partial\omega^2} > 0 \ . \tag{4.13}$$

The stable equilibria correspond to minima in ψ, the unstable equilibria to maxima. From equation (4.8) we see that the system is stable if and only if $\frac{dQ}{d\omega} < 0$. Hence the equilibria lying in fig. 6 between Z_1 and Z_2 on the dotted portion are unstable.

4.4 Adiabatic Stability

Now τ is essentially the resistive timescale; if we wish to consider relaxation on the frictional time scale we must introduce $s = p\tau$, and perturb as $\exp(\Gamma s)$ where $\Gamma = p^{-1}\gamma$. In terms of Γ, when $p \ll 1$ the dispersion relation reduces to

$$(\Gamma + 1)(16 + \omega_e^2) + 2S(16 - \omega_e^2) = 0 \ ,$$

or

$$\Gamma = -1 + \frac{2Q(\omega_e^2 - 16)}{(16 + \omega_e^2)^2} \tag{4.14}$$

$$= -\psi_{\omega\omega} .$$

This mode is one where resistivity is much stronger than friction and corresponds to the "adiabatic" relaxation discussed for the solid cylinder (cf. equation (3.9)).

4.5 Behaviour of Equilibria in the $(\omega_o - Q)$ control space

The rotation of a hollow annular shell has now been fully analysed and this system also possesses a simple cusp catastrophe, even though its potential (4.6) is not polynomial. The 'pucker point' in the (ω_o, Q, ω) space where the fold first develops is given by (4.7).

It is interesting to note that an alternative potential ψ_1 can be defined by

$$(16 + \omega^2)\ f(\omega) = -\frac{\partial\psi_1}{\partial\omega} \ , \tag{4.15}$$

(cf. eq. (2.18)), so that

$$\psi_1 = \tfrac{1}{4}\,\omega^4 - (1/3)\omega_o\omega^3 + (8 + Q)\omega^2 - 16\,\omega\omega_o \,. \qquad (4.16)$$

Using the transformation $\omega = (\omega_1 + \omega_o/3)$, we can remove the cubic term in the quartic for ω_1 to obtain the classical form for the elementary cusp catastrophe. At equilibria $\frac{\partial\psi_1}{\partial\omega} = 0 = \frac{\partial\psi}{\partial\omega}$ and $\frac{\partial^2\psi_1}{\partial\omega^2} = (16 + \omega^2)\,\frac{\partial^2\psi}{\partial\omega^2}$; maxima for ψ_1 correspond to maxima of ψ and similarly for minima. The functions ψ and ψ_1 thus have the same topology and this demonstrates clearly that ψ is the energy function for a simple cusp catastrophe.

5. DISCUSSION

5.1 Characteristics of Rotating Cylinders

In this paper we have taken Ω_o and B_o (or their non-dimensional counterparts ω_o and $Q^{\frac{1}{2}}$) as control variables, and examined the possible equilibria, ω_e, in the two limiting cases of a completely solid cylinder and a thin cylindrical solid shell. For sufficiently weak driving torques, ω_e decreases monotonically as the applied field is increased. For ω_o greater than some critical value ω_{oI}, a fold develops and the curve of ω_e against Q has the form shown in Fig. 6. The curve has an upper 'frictional' branch corresponding to stable fast rotation rates, and a lower 'magnetic' branch which gives stable slow rotation rates. Physically, the transition from the fast to the slow branch indicates that the onus of balancing the driving torque is passing from the frictional drag to the induced magnetic torque. The two branches overlap for $B_2 < B_o < B_1$ (say) so that in this range there are two distinct possible stable equilibrium rotation rates; which of these is realised in practice depends on whether B_o has been increased or decreased into this range. If B_o is increased through B_2, then the upper branch is followed until B_o equals B_1 at which point ω will jump 'discontinuously' down to the magnetic branch. Conversely, if B_o is decreased through B_1, then the lower branch is followed until B_o equals B_2, whereupon ω jumps up to the frictional branch. For our systems, the latter event appears to involve the larger change in ω_e. The fast and slow branches are separated by unstable equilibria (dotted in Fig. 6) so there exists a forbidden range in which no stable rotation rates are possible for <u>any</u> value of B_o (the annular shell, for instance, has a forbidden band $4 \lesssim \omega \lesssim \frac{1}{2}\omega_o$).

For both the solid cylinder and the annular cylindrical shell the induced magnetic torque about the axis of rotation increases linearly from zero with increasing ω, reaches a maximum and then falls to zero again as $\omega \to \infty$. This feature allows ω to be multi-valued for given control parameters ω_o and Q. The physical explanation for this effect seems to be that the rotation not only bends the field lines, producing the torque on the cylinder, but also expels them from the body of the cylinder. This leads eventually to both a drop in the Lorentz force and the formation of a 'surface' current density (Bullard 1949).

Skin effects are well known for A.C. currents flowing in solid conductors (see e.g. Shercliff 1965); in the frame of reference of the rotating object the steady applied magnetic field does appear as an A.C. field, so that such skin effects are not unexpected. Indeed in an induction motor, if ω is interpreted as the 'slip velocity' i.e. the departure of the cylinder angular velocity from that of the rotating field, then the magnetic torque is well known to depend on the slip in the fashion shown in Fig.1 (see e.g. Jayawant 1968).

Throughout this paper we have been concerned solely with the linear stability of our systems (i.e. stability to infinitesimal perturbations). The criteria found are then of course merely sufficient for instability and not, in general, sufficient for stability. Indeed, a glance at the potential functions of Fig. 3a leads us to expect finite amplitude instability when the system is in the fold region (or returning to the above notation when $B_2 < B_o < B_1$). Outside this range we might expect unconditional stability. Although we do not consider here the nature of any such subcritical instability, we note that the simple form of the controlling equations (4.10) for the annular shell makes such an investigation feasible (for a discussion of subcritical instability in the modified disc dynamo see Robbins (1977)).

5.2 Rotating Spheres

An analysis similar to that for the rotating cylinder can be carried out for a sphere of radius a rotating in vacuo in a transverse magnetic field $\underline{B}_o$. For this case we can express the magnetic field as

$$\underline{B} = \mathcal{R}e\left\{\mathrm{curl}\{\underline{R} \wedge \nabla(S(r,t)\sin\theta e^{i\phi})\}\right\} , \tag{5.1}$$

using spherical polar co-ordinates (R,θ,ϕ), and S is the appropriate complex poloidal scalar function (see R L Parker 1966). Introducing $s = S/aB_o$, the total magnetic torque about the axis of rotation is found to be

$$\mathcal{M} = \frac{4\pi a^3 B_o^2}{\mu} \mathcal{I}_m[s]_{r=1} , \tag{5.2}$$

with $s = s(r,t)$ and $R = ar$ (c.f. 2.12). If the sphere is replaced by a spherical shell of thickness δ this formula for $\mathcal{M}$ is unaffected, though the value of s at $r = 1$ is modified; in fact $\mathcal{M} \propto -\omega/(36 + \omega^2)$, $\omega = 2a\delta\Omega/\eta$, a functional form similar to that of a thin cylindrical annulus c.f. (4.5). (The retarding magnetic torques for thin spherical shell, cylindrical shell, and solid cylinder are given in Smythe (1950) pp.417-8, though in a less convenient form). For the solid sphere, the time independent solution is (Parker 1966, Bullard 1949)

$$s(r) = \frac{3}{2} \cdot \frac{r^{\frac{1}{2}} J_{3/2}(qr)}{(qr)J_{\frac{1}{2}}(q)} , \quad r \leq 1 , \tag{5.3}$$

where $q^2 = -i\omega$, and ω is the magnetic Reynolds number $\Omega a^2/\eta$ as for the solid cylinder. The Bessel functions of half integer order appearing in (5.3) can be expressed in terms of elementary functions (see e.g. Tranter 1968 p.12), and in particular we find

$$\mathfrak{Im}\,[s]_{r=1} = 3\left[\frac{1}{x^2} - \frac{1}{2x}\frac{(\sinh x + \sin x)}{(\cosh x - \cos x)}\right], \qquad (5.4)$$

where $x^2 = 2\omega$.

For the sphere, $\mathcal{M}$ varies linearly with ω for small ω, $\sim \omega^{-\frac{1}{2}}$ for $\omega \to \infty$, and possesses a maximum value as for the solid cylinder (it is illustrated in Fig. 6 of Bullard 1949 for n = m = 1 in his notation). The potential function characterising the equilibrium rotation rates is (c.f. 3.6).

$$\psi(\omega) = \tfrac{1}{2}\omega^2 - \omega\omega_o + \tfrac{1}{2} Q_s \ln\left(\frac{2(\cosh x - \cos x)}{x^2}\right), \qquad (5.5)$$

where Q_s is the analogue of the Q defined for the cylinder. This potential has the same topological features as those found for the cylinder, and so gives 'fast' and 'slow' branches with corresponding 'forbidden' bands of rotation rates.

5.3 Conditions for folded equilibria

The cusp catastrophe behaviour described for the cylinder and sphere appears to require a transverse applied magnetic field (i.e. one perpendicular to $\underline{\Omega}$). Bullard (1949) has calculated the torque on a solid sphere of radius a rotating in a uniform magnetic field $\underline{B}_o$ parallel to $\underline{\Omega}$ and concentrically embedded in a larger non-rotating sphere of radius a_1 and identical conductivity. The resulting torque about the axis of rotation is, in our notation

$$\mathcal{M} = \frac{2}{75} B_o^2 a^3 \omega\left(1 - \frac{a^5}{a_1^5}\right), \quad a_1 > a\ . \qquad (5.6)$$

This would give for the analogue of (2.17) $f(\omega) = \omega_o - \omega - Q_1\omega$ where Q_1 is appropriately defined, so that $\omega = \omega_o/(1 + Q_1)$ in equilibrium (in the absence of the external non-rotating shell the torque (5.6) vanishes). Since the torque is a linear function of ω over all the range with no maximum value, the ambiguity in the equilibrium rotation rate is removed, and the double branches and associated hysteresis are absent.

Moreover both friction and magnetic field are necessary to obtain the hysteresis. In the absence of the magnetic field, there is a simple stable equilibrium between driving torque and friction: $\omega = \omega_o$. In the absence of friction, the balance between driving and magnetic torques gives exactly two

equilibria (for the same Q) provided that the magnetic field strength exceeds some critical value B_{crit}. The slower of the two equilibria is stable while the faster is unstable (as the friction tends to zero, ω_o tends to infinity in Fig. 5, and we "lose" the frictional branch). For $B < B_{crit}$ the maximum magnetic torque is less than the driving torque, and the frictionless cylinder would accelerate indefinitely (as it would also do if started above the fast magnetic equilibrium branch mentioned above). For the annular cylindrical shell, B_{crit} corresponds to $Q = 4\omega_o$; this implies that the critical value of the magnetic field occurs when the energy of the applied field within the cylinder, $\pi a^2 L \left(\frac{B_o^2}{2\mu}\right)$, just equals the driving torque $\mathcal{T}$. For the solid sphere the maximum magnetic torque is $\sim V \left(\frac{B_o^2}{2\mu}\right)$ where V is the volume of the sphere.

Having shown that a compact body (the sphere) and an elongated body (the cylinder) both exhibit the folded catastrophe behaviour for the equilibrium rotation rate, we conjecture that any axisymmetric solid body or shell will display the same phenomenon when rotating in a uniform transverse magnetic field. In general, one can show that the magnetic torque can always be expressed in terms of surface integrals (see e.g. Herzenberg and Lowes). Moreover, one can consider the external induced field, and hence the surface integrals, as corresponding to dipole moments induced on the axis of rotation; the induced fields for spheres and cylinders have been calculated in this fashion by Landau and Lifschitz (1960,p.194).

We have considered a uniform transverse field; however any field with a transverse component seems likely to give a similar effect. Lin'kov and Urman (1974) have calculated magnetic torques on spheres for general inclined axisymmetric fields, and find that (except for parallel inclination where the torque is zero) all spherical harmonics produce torques that increase linearly in ω for small ω, reach a maximum, and decrease as $\omega^{-\frac{1}{2}}$ for $\omega \to \infty$. The maximum value of the torque is only weakly dependent on the order of the harmonic, although the angular velocity for which the maximum occurs does drift upwards (see their Fig. 1 for $\mathcal{I}m\,\chi_n(\kappa)$ in their notation).

We have carried out stability analyses for the totally solid cylinder ($p << 1$ gives explicit analytic results) and the thin cylindrical annulus, and find in both cases that the equilibria are defined by the turning points of a suitable potential function $\psi(\omega)$, i.e. when $\psi_\omega = 0$. The equilibria are found to be stable or unstable according as $\psi_{\omega\omega}$ is greater or less than zero. It seems likely that the general problem of computing the stability of axisymmetric rotators is reducible to this form, and that potential functions are obtainable in principle for all such bodies.

5.4 Non-linear friction

The analysis of this paper has been presented on the basis that the opposing frictional torque is linearly proportional to the rotation rate Ω. To check whether this assumption is crucial, we have investigated a more general form of the friction law - $\mathcal{F} \propto \Omega^{\varepsilon}$ where $\varepsilon > 0$. With a suitable renormalization of p and Q, the angular momentum equation becomes

$$p^{-1} \frac{d\omega}{d\tau} = \omega_o{}^{\varepsilon} - \omega^{\varepsilon} + \frac{1}{2} Q \beta_2 (1,\tau) \qquad (5.7)$$

(cf. 2.14). Introducing an appropriately modified potential function ψ, one can show that the condition for adiabatic stability remains $\psi_{\omega\omega} > 0$ at equilibrium values of ω. For the thin annulus, if $Q_\varepsilon \equiv 2Q/(\omega_o)^{\varepsilon}$, then the equation for equilibrium analogous to (4.5) is

$$Q_\varepsilon = \left(1 - \left(\frac{\omega}{\omega_o}\right)^{\varepsilon}\right)\left(\omega + \frac{16}{\omega}\right) \quad , \qquad (5.8)$$

from which evaluation of $\partial Q_\varepsilon/\partial\varepsilon$ shows that Q_ε is a monotonic increasing function of ε for fixed ω and ω_o. If then ε is varied in either direction away from unity the folded topology for sufficiently large ω_o remains. Indeed although $\partial Q_\varepsilon/\partial\omega < 0$ for $\omega < 4$, and for ω sufficiently close to ω_o, one can show that there always exists for sufficiently large ω_o a range of ω for which $\partial Q_\varepsilon/\partial\omega > 0$ even when ε approaches zero or infinity. As to the stability analysis for the thin annulus this follows through, provided $\varepsilon > 0$, without any change from that in §4.3 save that $(p^{-1}\gamma + 1)$ in equation (4.11) is replaced by $(p^{-1}\gamma + \varepsilon\, \omega_e{}^{\varepsilon-1})$, and $\psi_{\omega\omega}$ (or $\partial Q_\varepsilon/\partial\omega$) remains the discriminant. Q_ε itself is made up of two factors (see the r.h.s. of 5.8): the first is a monotonically decreasing function from one to zero at $\omega = \omega_o$; the second is an upward facing parabola-like curve which is the inverse of the magnetic torque curve. The product of two such factors will always produce a fold for sufficiently large ω_o, provided the magnetic torque curve has the characteristics we have already remarked on viz a maximum, and zero value as ω tends to zero and infinity. We conclude from this that the general features of the system we have discussed - fold, upper and lower stable branches, forbidden band of stable rotation rates - are not sensitive to the particular choice made for the friction law, provided the frictional torque increases monotonically with Ω.

5.5 Fluid Cylinders

The analysis of rotating fluid cylinders has not been carried out for a full range of magnetic Reynolds number. Weiss (1966, see his Fig.1) has performed numerical experiments for isolated eddies and finds expulsion of field for $\omega >> 1$. In this limit, the solid cylinder's equilibrium rotation rate satisfies $\omega_o - \omega - Q(2\omega)^{-\frac{1}{2}} = 0$, or

$$\omega \sim \omega_o - \frac{Q}{\sqrt{2}\,\omega_o^{\frac{1}{2}}} \tag{5.9}$$

(the asympotic value may be calculated from (3.5) using for example Tranter 1968 p.51). The annular cylindrical shell obeys

$$\omega \sim \omega_o - \frac{2Q}{\omega_o} \quad . \tag{5.10}$$

Moffatt (1965) treated the case of a cylinder filled with rotating viscous conducting fluid in a rotating applied field. He considered (in our notation) $\omega_o >> 1$, and $\omega_o - \omega << 1$ to obtain

$$\omega = \omega_o - \frac{Q}{4\omega_o} \tag{5.11}$$

for the (solid body rotating) inner core of the fluid. Thus when the magnetic field is concentrated in a skin at the edge of the conductor, the viscous fluid appears to behave (functionally) more like the annular shell, even though the fluid core rotates as a rigid body.

It is not possible here to say whether in the fluid case the transition from high to low ω or vice versa will be accompanied by the general behaviour we have found for rigid rotators. The vorticity generated in the fluid by the rotational part of the Lorentz force will distort the flow pattern and remove the axisymmetry from the system. The additional degrees of freedom might then enable the transition to be smoothed out and the hysteresis removed. However, large classes of bifurcating fluid equilibria have been found in many other non-magnetic systems (e.g. Platten and Chavepeyer 1975, Brooke Benjamin 1978).

5.6 Experimental Considerations

It is possible that the hysteresis in ω as a function of Q should be observable in the laboratory and experimentally verifiable. In principle, the values of Q obtainable are at the experimenter's disposal by suitable choice of the friction parameter λ of (2.13) (there is of course a lower limit

to λ in practice). The magnetic Reynolds number obtainable presents more of a problem. Table 1 shows approximate values of ω obtainable for solid cylinders and annular shells made of copper or aluminium.

	Solid Cylinder $a = 2.5$ cm.	Annular Shell $a = 2.5$ cm. $\delta = 0.25$ cm.
Copper	$4.9 \times 10^{-3}\ \Omega$	$9.8 \times 10^{-4}\ \Omega$
Aluminium	$3.1 \times 10^{-3}\ \Omega$	$6.2 \times 10^{-4}\ \Omega$

TABLE 1

Approximate values of magnetic Reynolds numbers ω (Ω in r.p.m.)

We see that for Ω = 5,000 r.p.m., ω for the solid copper cylinder is $\sim$ 25, and for the copper annulus $\omega \sim 5$. The regime of interest in each case is $\gtrsim$ 40 and $\gtrsim$ 20 respectively, so the attainable values appear a little low. However these values can be boosted in two ways. As $\omega \propto a^2$ for the solid cylinder and $\propto a\delta$ for the annulus, we could obviously increase ω by increasing the system dimensions. Secondly, there is the possibility of rotating the external applied field in a direction opposite to the sense of the driving torque. Rotating the external field is suggested for fluid systems in Moffatt (1965), and has been used for such systems experimentally (see Dahlberg 1972). If as seems likely the phenomena described in this paper survive the addition of rotating fields, then in principle the magnetic Reynolds number of the system can be easily lifted into the regime of interest.

6. CONCLUSIONS

When an axisymmetric electrically conducting solid body or shell is made to rotate, against friction, in a transverse magnetic field $\underline{B}_o$, the equilibrium rotation rate Ω is given by $\frac{\partial \psi}{\partial \omega} = 0$ where the potential function 'ψ' is given by (3.6) for a solid cylinder, (5.5) for a solid sphere and (4.6) for a thin cylindrical shell (the thin spherical shell has a similar form). For fixed friction coefficient there is in each case a minimum driving torque above which Ω is triple-valued for a range of values of B_o (see figure 6). For the thin cylindrical annulus which can be analysed completely, the upper and lower branches are stable against linear perturbations whilst the middle branch is unstable; this implies that for given friction and given driving torque there is a forbidden band of equilibrium rotation rates which are inaccessible however strong the applied magnetic field may be. For the solid cylinder we can prove similar stability properties when the ratio p of friction to magnetic diffusivity is small - the so-called 'adiabatic limit' - and numerical studies demonstrate these stability properties for general p. It is likely that these general features hold for all axisymmetric bodies and all values of p.

The development of this multi-valued 'folded' equilibrium rotation rate is an example of the cusp catastrophe of Thom, with ψ as the potential function. It appears to require a magnetic field with a component transverse to the rotation axis and is not sensitive to the form of the friction law provided friction increases monotonically with rotation rate. The folded nature of Ω results in hysteresis if the applied magnetic field strength is varied on a time scale long compared with all other time scales in the system. It is an interesting possibility that such hysteresis, which should be experimentally verifiable for solids, may be present for rotating fluids if the additional degrees of freedom do not smooth it away.

ACKNOWLEDGEMENTS

We thank Dr M Bevir for useful discussions and comments, and Dr M Proctor for a helpful discussion. We also thank T Martin and P S Jackson for assistance with the numerical investigation of (3.7). Some of this work (§3.1) was carried out when C.G.G. was a postgraduate student at Exeter University in receipt of a S.R.C grant. In this context he thanks Dr R Odoni for pointing out the identity (3.5).

PPENDIX 1

We here write down the general solution of equations (2.6, 2.7) for the on-dimensional magnetic stream function α and then show that only the m = 1 omponent contributes to the total magnetic torque on the rotating cylinder.

The general form of the solution of (2.6 and 2.7) can be expressed as

$$\left.\begin{aligned} \alpha &= \mathcal{R}e\,(re^{i\theta} + \sum_{m=1}^{\infty} b_m(\tau) r^{-m} e^{im\theta}) \qquad r \geqslant 1\ , \\ &= \mathcal{R}e\,(\sum_{m=1}^{\infty} c_m(\tau) r^{m} e^{im\theta}) \qquad , 0 \leqslant r \leqslant k\ , \\ &= \mathcal{R}e\,(\sum_{m=1}^{\infty} d_m(r,\tau) e^{im\theta}) \qquad , k \leqslant r \leqslant 1\ , \end{aligned}\right\} \tag{A.1}$$

here the b_m, c_m and d_m are in general complex, and $\mathcal{R}e$ denotes real part. he boundary conditions are that the uniform field must be recovered as $r \to \infty$, hat $\underline{B}$ is finite, and that $\underline{B}$ is continuous across the surfaces of the annulus. In terms of α we have $\alpha \to \mathcal{R}e\,(re^{i\theta})$ as $r \to \infty$, α finite, and both α and $\frac{\partial \alpha}{\partial r}$ are continuous at r = ka and a. The first two conditions have been used in writing α in the form (A.1); the latter conditions lead to

$$\left.\begin{aligned} & mc_m(\tau)\, k^m = md_m(k,\tau) = k\left(\frac{\partial}{\partial r} d_m(r,\tau)\right)_{r=k}, \quad \text{for all } m\ , \\ & mb_m(\tau) = md_m(1,\tau) = -\left(\frac{\partial}{\partial r} d_m(r,\tau)\right)_{r=1} \quad , \quad \text{for } m \neq 1\ , \\ & b_1(\tau) = d_1(1,\tau) - 1 = 1 - \left(\frac{\partial}{\partial r} d_1(r,\tau)\right)_{r=1}. \end{aligned}\right\} \tag{A.2}$$

The moment exerted by the Lorentz force on an element of the annulus is $\underline{d\mathcal{M}} = \underline{R} \wedge \underline{dF}$ where $\underline{dF} = \mu^{-1}\ (\text{curl}\ \underline{B}) \wedge \underline{B}\ RdRd\theta d\bar{z}$. Hence the total magnetic torque over the whole of the annulus is

$$\underline{\mathcal{M}} = -\hat{\underline{z}}\, \mu^{-1} \int_0^L \int_{ka}^{a} \int_0^{2\pi} R\, \frac{\partial A}{\partial \theta}\, \nabla^2 A\, d\theta dR d\bar{z},$$

or using dimensionless variables

$$\mathcal{M} = -\frac{(B_o^{\,2}\, La^2)}{\mu} \int_0^{'} \int_k^{'} \int_0^{2\pi} r\, \frac{\partial \alpha}{\partial \theta}\, \nabla^2 \alpha\, d\theta dr dz\ . \tag{A.3}$$

Inserting (A.1(iii)) into (A.3), it follows on integrating with respect to θ that no cross terms occur in the torque. Integrating with respect to r by parts then gives only surface contributions:-

$$\mathcal{M} = -\left(\frac{\pi B_o^2 La^2}{\mu}\right) \mathfrak{Im} \sum_{m=1}^{\infty} \left\{ \left(d_m^* \frac{\partial d_m}{\partial r} \right)_{r=1} - \left(k d_m^* \frac{\partial d_m}{\partial r} \right)_{r=k} \right\}, \qquad (A.4)$$

where $\mathfrak{Im}$ denotes imaginary part, and * signifies complex conjugate. From (A.2) however, $\{d_m^* \frac{\partial}{\partial r}(d_m)\}_{r=k} = mk^{2m-1} c_m c_m^*$ for all m, which is a real quantity. Similarly, $\{d_m^* \frac{\partial}{\partial r}(d_m)\}_{r=1} = -m b_m^* b_m$ for $m \neq 1$, and this is also real. Thus the magnetic torque has a non-zero contribution only from the $m = 1$ component of α, and that from the outer surface of the annulus alone. Hence we need not consider modes with $m \neq 1$ when analysing the stability of the cylinder's rotation.

REFERENCES

Brooke Benjamin T, 1978, Proc. Roy. Soc. A, 359, 1.

Bullard E C, 1949, Proc. Roy. Soc. A, 199, 413.

Busse F H, 1975, J. Fluid Mech., 71, 193.

Clark A, 1965, Phys. Fl., 8, 644.

Dahlberg E, 1972, AB Atomenergi, Sweden, Rep. AE-447.

Devanathan C and Bhatnagar P L, 1967, Proc. Roy. Soc. A, 297, 558.

Galloway D J, Proctor M R E and Weiss N O, 1977, Nature, 266, 686.

Galloway D J, Proctor M R E and Weiss N O, 1978, In Press.

Gimblett C G, 1977, Ph.D. Thesis, Exeter University.

Herzenberg A and Lowes F J, 1957, Phil. Trans. A, 249, 507.

Jayawant B V, 1968, "Induction Machines", McGraw-Hill

Landau L D and Lifshitz E M, 1960, "Electrodynamics of Continuous Media", Pergamon Press.

Lin'Kov R V and Urman Yu.M., 1974, Sov. Phys. Tech. Phys., 18, 1557.

Moffatt H K, 1965, J. Fluid Mech., 22, 521.

Parker E N, 1963, Astrophysical J., 138, 552.

Parker R L, 1966, Proc. Roy. Soc. A., 291, 60.

Peckover R S and Weiss N O, 1978, Mon. Not. R. Astr. Soc., 182, 189.

Platten J K and Chavepeyer G, 1975, Int. J. Heat Mass Transfer, 18, 1071.

Richardson A T, 1974, J. Fluid Mech., 63, 593.

Robbins K A, 1977, Math. Proc. Camb. Phil. Soc., 82, 309.

Shercliff J A, 1965, 'A Textbook of Magnetohydrodynamics', Pergamon Press.

Smythe W R, 1950, 'Static and Dynamic Electricity', McGraw-Hill.

Thom R, 1975, 'Structural Stability and Morphogenesis', W A Benjamin.

Thonemann P C and Kolb A C, 1964, Phys. Fluids, 7, 1455.

Tranter C J, 1968, 'Bessel Functions with some Physical Applications', English Universities Press.

Weiss N O, 1964, Phil. Trans. A, 256, 99.

Weiss N O, 1966, Proc. Roy. Soc. A, 293, 310.

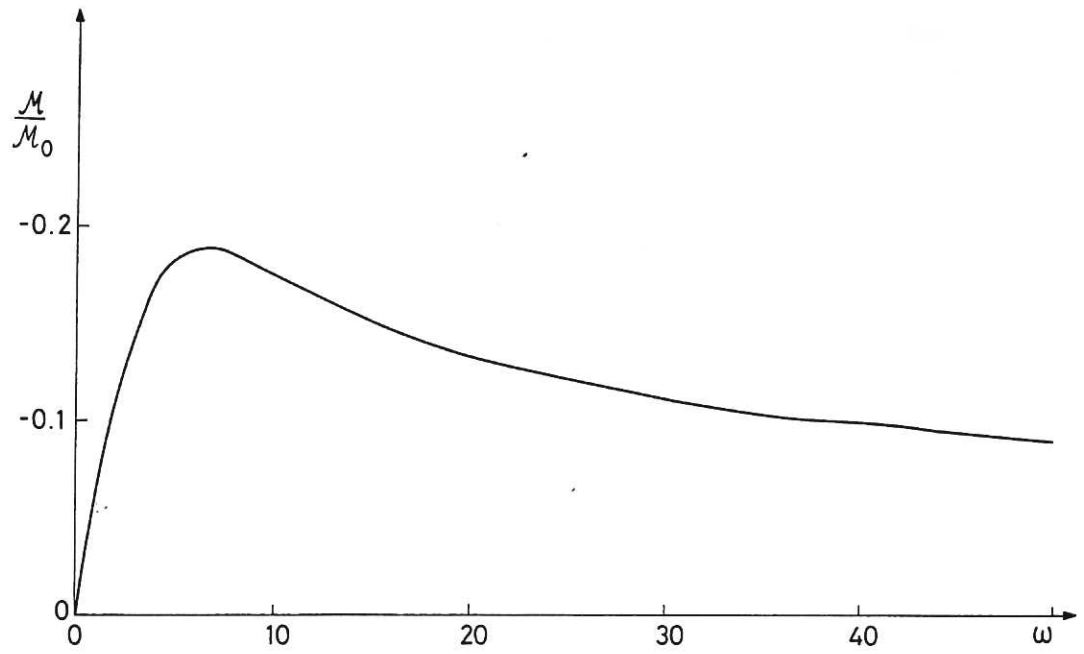

Fig.1 The induced magnetic torque $\mathcal{M}$ for a solid cylinder rotating in a transverse magnetic field plotted as a function of the non-dimensional rotation velocity ω (see eq.3.3). The scaling factor $\mathcal{M}_0 = 4(\pi B_0^2 La^2/\mu)$ is proportional to the magnetic energy within the cylinder at rest.

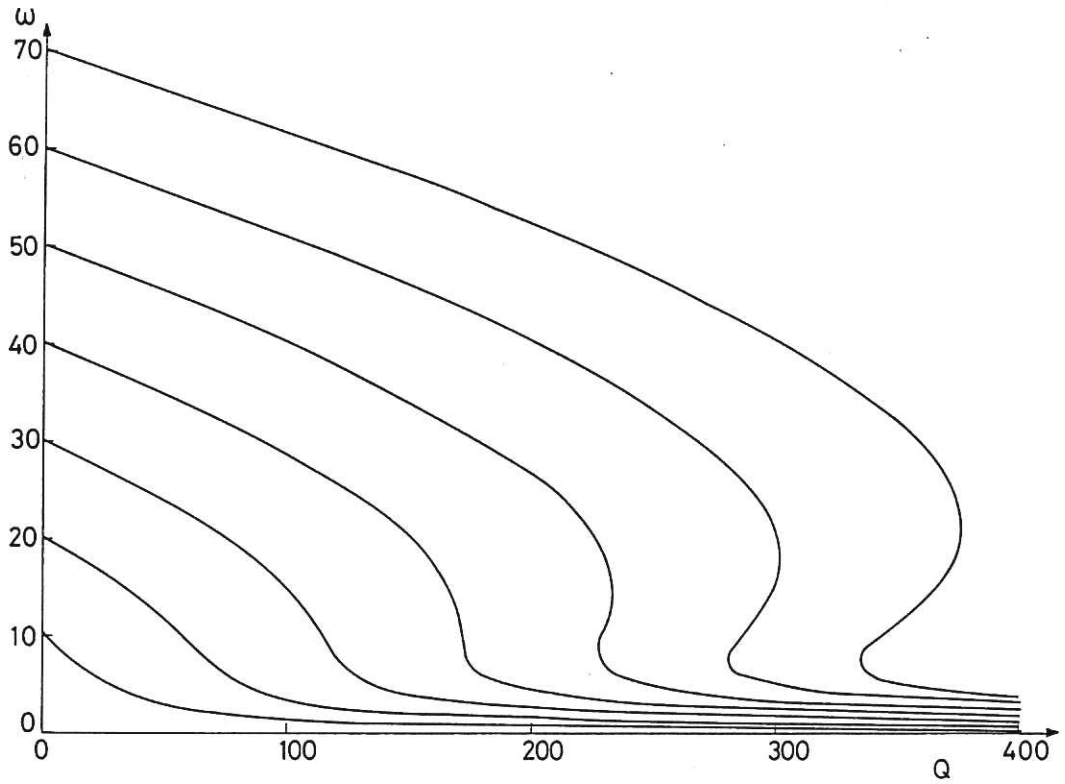

Fig.2 Equilibrium (dimensionless) rotation rates ω plotted against Q for various values of ω_0 for the solid cylinder (see eq.3.4). The re-entrant 'knee' develops for all loci which have $\omega_0 > 42{\cdot}3$.

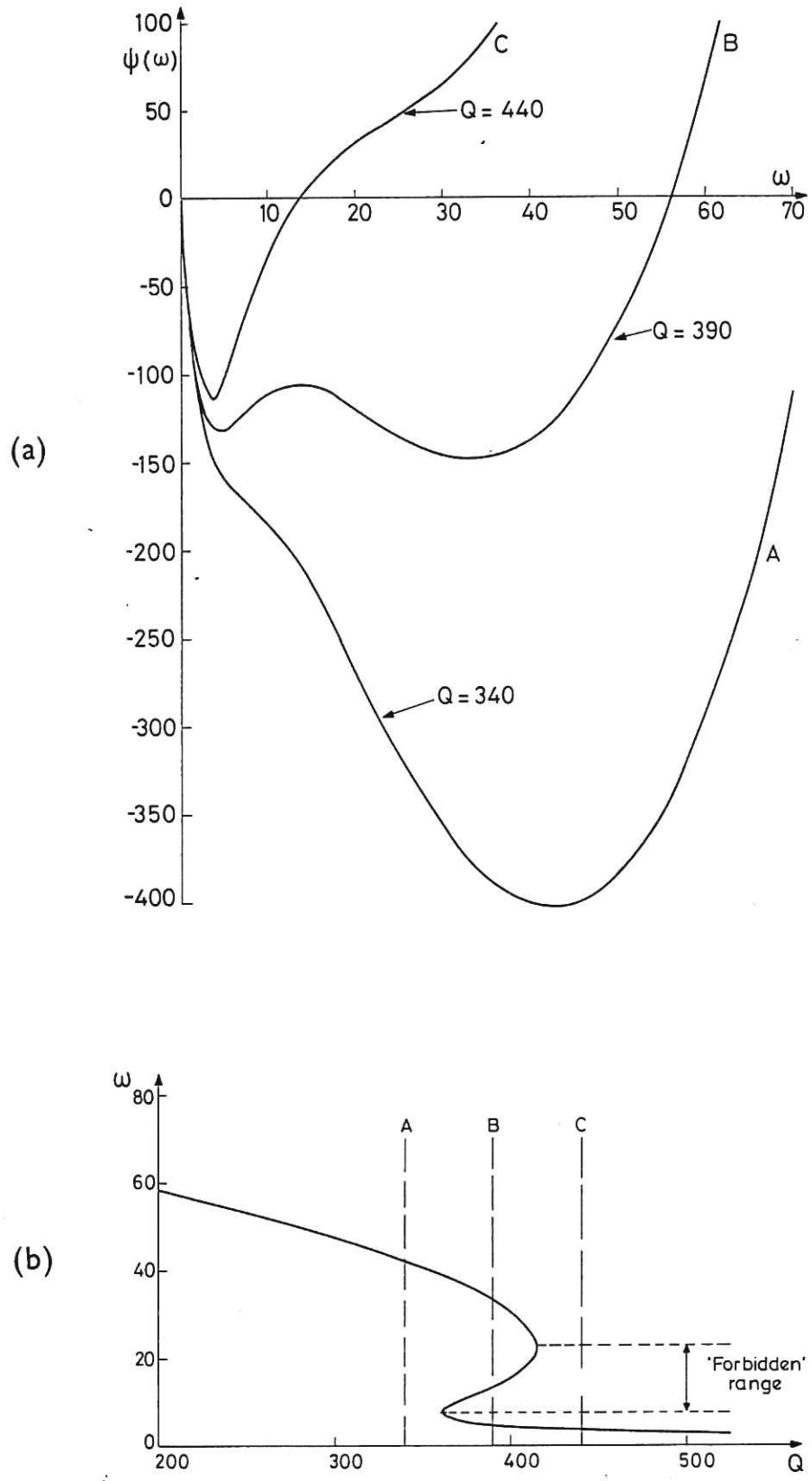

Fig.3(a) Plots for the solid cylinder of the 'energy' function $\psi(\omega)$ (see eq.3.6) for $\omega_0 = 75$ and 3 different values of Q in the vicinity of the fold. (b) The cross-sectional cuts in the $(\omega-Q)$ plane to which the three forms of ψ in 3(a) correspond. The curve shown is $\omega = \omega(Q)$ for $\omega_0 = 75$. The part of the curve in the 'forbidden' range is unstable and corresponds to a local maximum in ψ e.g. in B in 3(a).

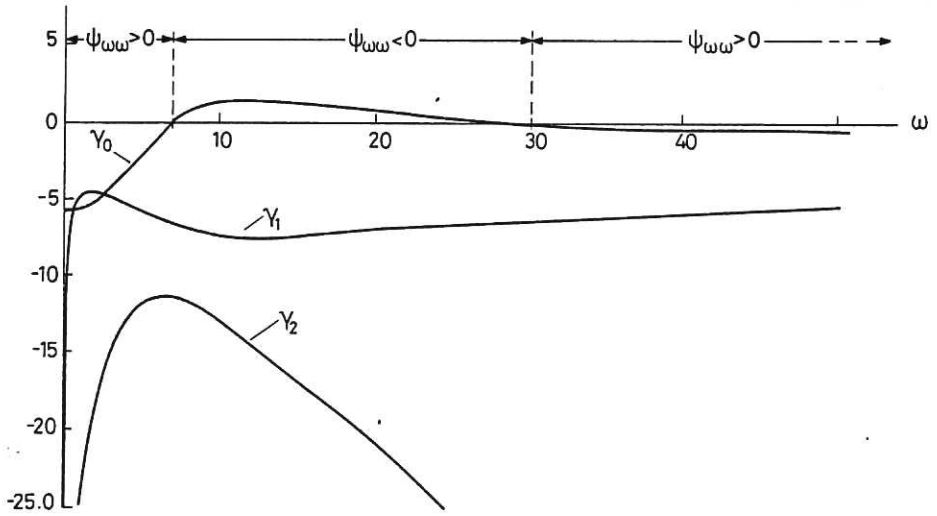

Fig.4 The roots of the dispersion relation (3.7) for the solid cylinder when $\omega_0 = 100$ and $p = 1$. γ_0 is the real root which is positive when $\psi_{\omega\omega} < 0$ and negative otherwise. The two complex roots are $\gamma_1 \pm i\gamma_2$ which give highly damped, high frequency oscillations.

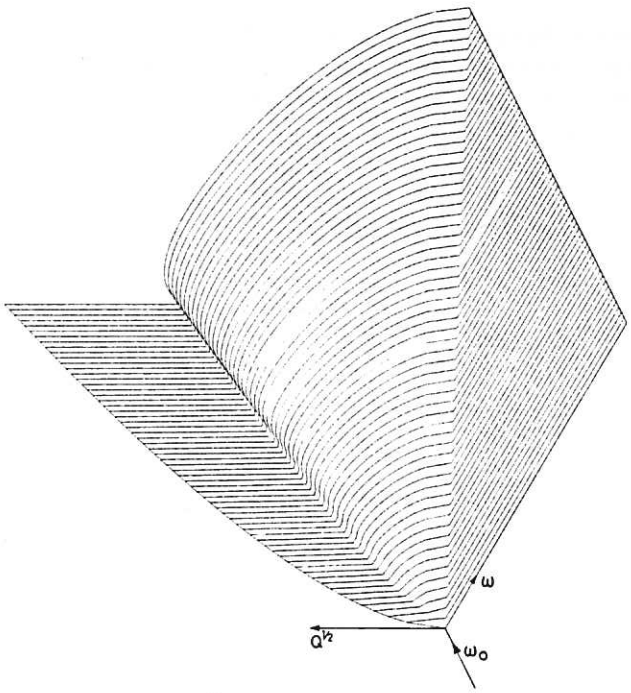

Fig.5 Three-dimensional plot of the developing fold in $(\omega_0, Q^{1/2}, \omega)$ space for the solid cylinder. In the vicinity of the origin the fold is not re-entrant. The 'pucker' point is at $\omega_0 = 42{\cdot}3 \quad \omega = 10{\cdot}7 \quad Q = 185{\cdot}1$.

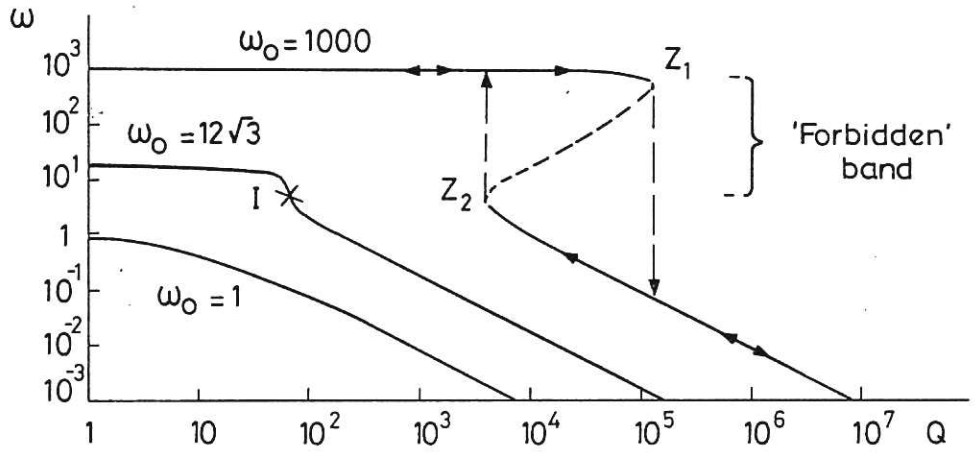

Fig.6 Schematic plots for the annular cylindrical shell of the (dimensionless) equilibrium rotation rate ω as a function of Q for 3 different dimensionless driving torques ω_o (see eq.4.5) (i) $\omega_o = 1000$ – the dashed part of the curve represents the unstable equilibria; the arrows indicate the course taken as Q is slowly increased or decreased. The (ω, Q) co-ordinates of the turning points are $Z_1 \simeq (\omega_o/2, \omega_o^2/8)$ and $Z_2 \simeq (4, 4\omega_o)$. (ii) $\omega_o = 12\sqrt{3}$ – this curve contains the 'pucker' point I ($\omega_I = 4\sqrt{3}$, $Q_I = 64$) at which $dQ/d\omega = 0$. Above this curve all equilibrium curves have an unstable portion of which (i) is typical; below (ii) no curves have folds (iii) $\omega_o = 1$ – a simple monotonically decreasing curve, with $\omega \propto Q^{-1}$ for large Q.